

Joint Transmit and Receive Beamforming for Multi-Relay MIMO-OFDMA Cellular Networks

Kent Tsz Kan Cheung, Shaoshi Yang and Lajos Hanzo

School of ECS, University of Southampton, SO17 1BJ, United Kingdom.

Email: {ktkc106,sy7g09,lh}@ecs.soton.ac.uk, wireless.ecs.soton.ac.uk

Abstract—A novel transmission protocol is conceived for a multi-user, multi-relay, multiple-input–multiple-output orthogonal frequency-division multiple-access (MIMO-OFDMA) cellular network based on joint transmit and receive beamforming. More specifically, the network’s MIMO channels are mathematically decomposed into several effective multiple-input–single-output (MISO) channels, which are spatially multiplexed for transmission. For the sake of improving the attainable capacity, these MISO channels are grouped using a pair of novel grouping algorithms, which are then evaluated in terms of their performance versus complexity trade-off¹.

I. INTRODUCTION

Recent wireless mobile broadband standards optionally employ relay nodes (RNs) and multiple-input–multiple-output orthogonal frequency-division multiple-access (MIMO-OFDMA) systems [2], [3] for supporting the ever-growing wireless capacity demands. These systems benefit from a capacity gain increasing roughly linearly both with the number of available OFDMA subcarriers (each having the same bandwidth) as well as with the minimum of the number of transmit antennas (TAs) and receive antennas (RAs). However, given the additional resources, the issue arises as to how best to allocate them for maximizing the system’s capacity. In light of these discussions, we propose a novel joint transmit and receive beamforming (BF) protocol for coordinating the downlink (DL) transmissions in a sophisticated multi-relay aided MIMO-OFDMA cellular network.

It is widely acknowledged that under the idealized simplifying condition of having perfect channel state information (CSI) at the transmitter, the DL or broadcast channel (BC) capacity [4], [5] may be approached with the aid of dirty paper coding (DPC) [6]. However, the practical implementation of DPC is hampered by its excessive algorithmic complexity upon increasing the number of users. On the other hand, BF is an attractive suboptimal strategy for allowing multiple users to share the BC while resulting in reduced multi-user interference (MUI). A low-complexity transmit-BF technique is the zero-forcing based BF (ZFBBF), which can asymptotically achieve the BC capacity as the number of users tends to infinity [7]. Furthermore, ZFBBF may be readily applied to a system with multiple-antenna receivers through the use of the singular value decomposition (SVD). As a result, the associated MIMO channels may be mathematically decomposed into several effective multiple-input–single-output (MISO) channels, which are termed spatial multiplexing components (SMCs) in this work.

In [8], these SMCs are specifically grouped so that the optimal grouping as well as the optimal allocation of the power may be found on each subcarrier block using convex optimization. In contrast to the channel-diagonalization methods

of [9]–[11], the ZFBBF approach does not enforce any specific relationship between the total numbers of TAs and RAs. Therefore, ZFBBF is more suitable for practical systems, since the number of TAs at the BS is typically much lower than the total number of RAs of all the active user equipments (UEs). Compared to the random beamforming methods, such as that of [12], ZFBBF is capable of completely avoiding the interference, thus improving the system’s attainable capacity.

Due to its desirable performance versus complexity trade-off, in this paper we employ ZFBBF in the context of multi-relay aided MIMO-OFDMA systems, where the direct link between the base station (BS) and the UE may be exploited in conjunction with the relaying link for further improving the system’s performance.

In this paper, we propose a novel transmission protocol for a generalized multi-user multi-relay aided MIMO-OFDMA cellular system, which supports simultaneous direct and relayed transmissions without imposing interference on the receivers. This is accomplished by mathematically decomposing the network’s channel matrices for ensuring that the beneficial links may be grouped for simultaneous transmission. The system model in [7], [8], [13], [14] is improved, since these contributions did not consider exploiting relaying for improving the system’s performance, or only considered single-relay, single-user scenarios. Furthermore, we imposed no constraint on the relationship between the number of TAs and RAs in the system, which was assumed in [9]–[11].

Furthermore, we conceive a pair of novel algorithms for grouping the SMCs transmissions. These challenging issues of two-phase communication in the presence of multiple transmitters as well as simultaneous direct and relayed transmissions are resolved by the proposed grouping algorithms. The first grouping algorithm is optimal in the sense that it is based on exhaustive search over all the SMC groupings that satisfy the semi-orthogonality criterion, while the second algorithm constitutes a lower-complexity alternative. In terms of its basic principle, the lower-complexity method is reminiscent of [7], [8], but it has been appropriately adapted for the multi-relay cellular network considered.

II. SYSTEM MODEL

We focus our attention on the DL of a multi-relay MIMO-OFDMA cellular network, as shown in Fig. 1. The BS, M RNs and K UEs are each equipped with N_B , N_R and N_U antennas, respectively. The cellular system has access to N subcarrier blocks, each encompassing W Hertz of wireless bandwidth. The subcarrier blocks considered here are similar to the resource blocks in the LTE-nomenclature [15]. The BS is located at the cell-center, while the RNs are each located at a fixed distance from the BS and are evenly spaced around it. On the other hand, the UEs are uniformly distributed in the cell. The BS coordinates and synchronizes its own

¹This paper concisely focuses on the transmission protocol proposed in our previous work [1]. For more details, please refer to [1].

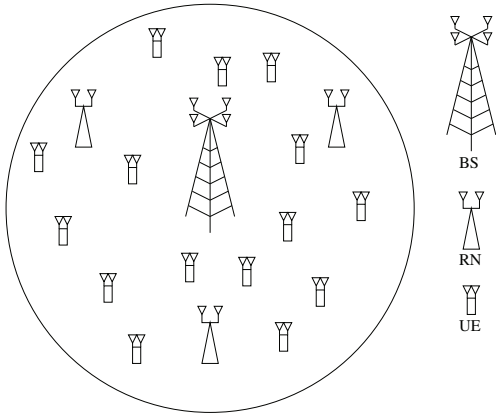


Fig. 1: An example of a multi-relay MIMO-OFDMA cellular network, containing a BS at the cell-center, 3 RNs and 15 UEs.

transmissions with that of the RNs, which employ the decode-and-forward (DF) [16] transmission protocol and thus avoids the problem of noise amplification.

For the subcarrier block $n \in \{1, \dots, N\}$, let us define the complex-valued wireless channel matrices between the BS and UE $k \in \{1, \dots, K\}$, between the BS and RN $m \in \{1, \dots, M\}$, and between RN m and UE k as $\mathbf{H}_{n,k}^{BU} \in \mathbb{C}^{N_U \times N_B}$, $\mathbf{H}_{n,m}^{BR} \in \mathbb{C}^{N_R \times N_B}$ and $\mathbf{H}_{n,m,k}^{RU} \in \mathbb{C}^{N_U \times N_R}$, respectively. These complex-valued channel matrices account for both the frequency-flat Rayleigh fading and the path-loss between the corresponding transceivers. The coherence bandwidth of each wireless link is assumed to be sufficiently high, so that each individual subcarrier block experiences frequency flat fading, although the level of fading may vary from one subcarrier block to another in each transmission period. Additionally, the transceivers are stationary or moving slowly enough so that the level of fading may be assumed to be fixed for the duration of a scheduled transmission period. Furthermore, the RAs are spaced sufficiently far apart, so that each TA/RA pair experiences independent and identically distributed (i.i.d.) fading. Since these channels are slowly varying, the system is capable of exploiting the benefits of channel reciprocity associated with time-division duplexing (TDD) as well as dedicated low-rate error-free feedback channels, so that the CSI becomes available at each BS- and RN-transmitter as well as at each possible RN- and UE-receiver. It is assumed that the BS performs network-wide scheduling and that these channel matrices have full row rank, which may be achieved with a high probability for typical DL wireless channel matrices.

Furthermore, each receiver suffers from additive white Gaussian noise (AWGN) having a power spectral density of N_0 . The maximum instantaneous transmission power available to the BS and to each RN due to regulatory and health-constraints is P_{max}^B and P_{max}^R , respectively. Since OFDMA modulation constitutes a linear operation, we focus our attention on a single subcarrier block and as usual, we employ the commonly-used equivalent baseband signal model

III. TRANSMISSION PROTOCOL DESIGN

The system can simultaneously use two transmission modes to convey information to the UEs, namely the BS-to-UE mode, and the relaying-based BS-to-RN and RN-to-UE mode. Note that although in classic OFDMA each data stream is orthogonal in frequency, for the sake of further improving the system's attainable performance, our system employs spatial multiplexing in conjunction with ZFBF so that multiple data

streams may be served using the same subcarrier block, without suffering from interference. Additionally, since the relaying-based transmission can be split into two phases, the design philosophy of the BF matrices in each phase are described separately, although for simplicity we have assumed that the respective channel matrices remain unchanged in both phases. Firstly, the definition of the semi-orthogonality criterion is given as follows [7].

Definition 1. A pair of MISO channels, represented by the complex-valued column vectors \mathbf{v}_1 and \mathbf{v}_2 , are said to be semi-orthogonal to each other with parameter $\alpha \in [0, 1]$, when²

$$\frac{|\Re(\mathbf{v}_1^H \mathbf{v}_2)|}{\|\mathbf{v}_1\| \|\mathbf{v}_2\|} \leq \alpha. \quad (1)$$

To be more specific, a measure of the grade of orthogonality between \mathbf{v}_1 and \mathbf{v}_2 is given by the left-hand side of inequality (1), which ranges from 0 for orthogonal vectors to 1 for linearly dependent vectors.

The authors of [7] demonstrated that employing the ZFBF strategy for MISO channels that satisfy $\alpha \rightarrow 0$, while the number of users obeys $K \rightarrow \infty$, asymptotically achieves the DPC capacity, and it is therefore optimal for the BC channel. Similar principles are followed in this paper.

A. BF design for the first transmission phase

In the first transmission phase, only the BS is transmitting, while both the RNs and the UEs act as receivers. This is similar to the classic DL multi-user MIMO model. As described above, our aim is 1) to design a ZFBF matrix for the BS to avoid interference between data streams, and 2) to design receive BF matrices for the UEs and RNs so that the resultant *effective DL channel matrices* contain as many semi-orthogonal rows as possible that satisfy (1) for a given α . Ideally, a joint computation of the receive BF matrices is performed for satisfying the latter condition. However, this is generally impossible due to the geographically distributed nature of the UEs and RNs. Instead, we opt for a compromise by employing the SVD, so that at least each individual effective DL channel matrix contains orthogonal rows.

Bearing this in mind, the channel matrices of all DL transmissions originating from the BS are decomposed at the BS, UEs and RNs using the SVD as $\mathbf{H}_{n,k}^{BU} = \mathbf{U}_{n,k}^{BU} \mathbf{S}_{n,k}^{BU} (\mathbf{V}_{n,k}^{BU})^H$ and $\mathbf{H}_{n,m}^{BR} = \mathbf{U}_{n,m}^{BR} \mathbf{S}_{n,m}^{BR} (\mathbf{V}_{n,m}^{BR})^H$, respectively. Thus, the receive-BF matrices for UE k and RN m are given by $\mathbf{R}_{n,k}^{BU,T_1} = (\mathbf{U}_{n,k}^{BU})^H$ and $\mathbf{R}_{n,m}^{BR,T_1} = (\mathbf{U}_{n,m}^{BR})^H$, and the effective DL channel matrices are then given³ by $\underline{\mathbf{H}}_{n,k}^{BU,T_1} = \mathbf{R}_{n,k}^{BU,T_1} \mathbf{H}_{n,k}^{BU} = \mathbf{S}_{n,k}^{BU} (\mathbf{V}_{n,k}^{BU})^H$ and $\underline{\mathbf{H}}_{n,m}^{BR,T_1} = \mathbf{R}_{n,m}^{BR,T_1} \mathbf{H}_{n,m}^{BR} = \mathbf{S}_{n,m}^{BR} (\mathbf{V}_{n,m}^{BR})^H$, respectively. Since $\mathbf{V}_{n,k}^{BU}$ and $\mathbf{V}_{n,m}^{BR}$ are both unitary, while $\mathbf{S}_{n,k}^{BU}$ and $\mathbf{S}_{n,m}^{BR}$ are both real and diagonal, these effective DL channel matrices respectively consist of $\min(N_B, N_U)$ and $\min(N_B, N_R)$ orthogonal non-zero rows with norms equal to their corresponding singular values. We refer to these non-zero orthogonal rows as the SMCs of their associated MIMO channel matrix. The K BS-to-UE MIMO channel

²In this paper, $\Re(x)$ denotes the real component of x .

³Note that T_1 is used for indicating the first transmission phase, and underline is used to denote the effective DL channel matrices.

matrices and M BS-to-RN channel matrices generate a total of $[K \cdot \min(N_B, N_U) + M \cdot \min(N_B, N_R)]$ SMCs. Since these SMCs are generated from independent MIMO channel matrices associated with geographically distributed UEs and RNs, they are not all guaranteed to be orthogonal to each other. Furthermore, since each UE or RN has multiple antennas and N_B might not be sufficiently large to simultaneously support all UEs and RNs, we have to determine which specific SMCs should be selected. As a result, for each two-phase transmission period, we opt for selecting a SMC group accounting for both phases from the set of available SMC groups. The generation of SMC groups is accomplished by the SMC grouping algorithms to be described in Section IV.

To elaborate a little further, a set of SMC groups, \mathcal{G}_n , which is associated with subcarrier block n , may be obtained using one of the grouping algorithms presented in Section IV. The BS selects a single group, $j \in \mathcal{G}_n$, containing (but not limited to⁴) $Q_j^{T_1}$ SMCs out of the $[K \cdot \min(N_B, N_U) + M \cdot \min(N_B, N_R)]$ available SMCs to be supported by using ZFBF. Thus, we have $Q_j^{T_1} \leq \min[N_B, K \cdot \min(N_B, N_U) + M \cdot \min(N_B, N_R)]$ and a multiplexing gain of $Q_j^{T_1}$ is achieved. Let us denote the refined effective DL channel matrix with rows being the $Q_j^{T_1}$ selected SMCs as $\underline{\mathbf{H}}_{n,j}^{T_1} \in \mathbb{C}^{Q_j^{T_1} \times N_B}$. The ZFBF transmit matrix applied at the BS to subcarrier block n is then given by the following right inverse $\mathbf{T}_{n,j}^{T_1} = \left(\underline{\mathbf{H}}_{n,j}^{T_1} \right)^H \cdot \left[\underline{\mathbf{H}}_{n,j}^{T_1} \left(\underline{\mathbf{H}}_{n,j}^{T_1} \right)^H \right]^{-1}$. Since $\underline{\mathbf{H}}_{n,j}^{T_1} \mathbf{T}_{n,j}^{T_1} = \mathbf{I}_{N_B}$, the potential interference between the $Q_j^{T_1}$ selected SMCs is completely avoided. Furthermore, the columns of $\mathbf{T}_{n,j}^{T_1}$ are normalized by multiplying the diagonal matrix $\mathbf{W}_{n,j}^{T_1}$ on the right-hand side of $\mathbf{T}_{n,j}^{T_1}$ to ensure that each SMC transmission is initially set to unit power.

Then, $\mathbf{T}_{n,j}^{T_1} \mathbf{W}_{n,j}^{T_1}$ is used as the DL transmit-BF matrix for the BS in the first phase. Thus, the effective channel-to-noise ratios (CNRs) in the first transmission phase can be written as $G_{n,j,e_1}^{BU,T_1} = |w_{n,j,e_1}^{BU,T_1}|^2 / \Delta\gamma N_0 W$ and $G_{n,j,e}^{BR,T_1} = |w_{n,j,e}^{BR,T_1}|^2 / \Delta\gamma N_0 W$, respectively, where w_{n,j,e_1}^{BU,T_1} and $w_{n,j,e}^{BR,T_1}$ are the diagonal elements in $\mathbf{W}_{n,j}^{T_1}$, $\Delta\gamma$ is the signal-to-noise ratio (SNR) gap, and noise power received on each subcarrier block is given by $N_0 W$. More specifically, these diagonal elements correspond to SMC group j and subcarrier block n , and they are associated with either a direct BS-to-UE SMC or a BS-to-RN SMC. The additional subscripts $e_1 \in \{0, \dots, \min[N_B, K \cdot \min(N_B, N_U)]\}$ and $e \in \{0, \dots, \min[N_B, M \cdot \min(N_B, N_R), K \cdot \min(N_R, N_U)]\}$ are used for distinguishing the multiple selected SMCs of the direct links (i.e. those related to UEs), from the multiple selected SMC-pairs⁵ that may be associated with a particular RN $\mathcal{M}(e)$, respectively. Note that $\mathcal{M}(e)$ is a function of e , representing the RN index (similar to m used before) associated with the SMC-pair e , as further detailed in Section IV.

⁴The SMC group selection, as a part of the scheduling operation, is carried out at the BS before initiating the first transmission phase. Hence, the selected SMC group will also contain $Q_j^{T_2}$ SMCs selected by the BS for the second transmission phase, as detailed in Section III-B.

⁵A single SMC-pair consists of a SMC for the first phase and another for the second phase. Although these SMCs are generated separately in each phase, the SMC-pair associated with a common RN has to be considered as a single entity in the SMC grouping algorithms presented in Section IV.

B. BF design in the second transmission phase

The second transmission phase may be characterized by the *MIMO interference channel*. A similar methodology is employed in the second transmission phase, except that now both the BS and the RNs are transmitters, while a number of UEs are receiving. In this phase, our aim is 1) to design ZFBF matrices for the BS and RNs to avoid interference between data streams, 2) and to design a receive-BF matrix for each UE so that the effective channel matrices associated with each of its transmitters contain rows which satisfy the semi-orthogonal condition (1) for a given α . This means that more data streams may be served simultaneously, thus improving the attainable system performance. Since there are multiple *distributed* transmitters/MIMO channel matrices associated with each UE, the SVD method described in Section III-A, which is performed in a centralized fashion, cannot be readily applied at the transmitter side. Instead, we aim for minimizing the resultant correlation between the generated SMCs, thus increasing the number of SMCs which satisfy (1) for a given α . To accomplish this goal, we begin by introducing the shorthand of $\underline{\mathbf{H}}_{n,k}^{BU,T_2} = \mathbf{R}_{n,k}^{U,T_2} \mathbf{H}_{n,k}^{BU}$ and $\underline{\mathbf{H}}_{n,m,k}^{RU,T_2} = \mathbf{R}_{n,k}^{U,T_2} \mathbf{H}_{n,m,k}^{RU}$ as the effective channel matrices between the BS and UE k , and between RN m and UE k , respectively, on subcarrier block n in the second transmission phase, where $\mathbf{R}_{n,k}^{U,T_2}$ is the yet-to-be-determined UE k 's receive-BF matrix. In light of the preceding discussions, one of our aims is to design $\mathbf{R}_{n,k}^{U,T_2}$ so that the off-diagonal values of the matrices given by $\mathbf{A}_0 = \underline{\mathbf{H}}_{n,k}^{BU,T_2} \left(\underline{\mathbf{H}}_{n,k}^{BU,T_2} \right)^H$ and $\mathbf{A}_m = \underline{\mathbf{H}}_{n,m,k}^{RU,T_2} \left(\underline{\mathbf{H}}_{n,m,k}^{RU,T_2} \right)^H$, $\forall m$ are as small as possible. This design goal may be formalized as

$$\min_{\mathbf{R}_{n,k}^{U,T_2}} \left\| \left\| \underline{\mathbf{H}}_{n,k}^{BU} \left(\underline{\mathbf{H}}_{n,k}^{BU} \right)^H - \left(\mathbf{R}_{n,k}^{U,T_2} \right)^{-1} \mathbf{\Lambda}_0 \left(\mathbf{R}_{n,k}^{U,T_2} \right)^{-H} \right\|_{\mathbb{F}}^2 + \sum_{m=1}^M \left\| \left\| \underline{\mathbf{H}}_{n,m,k}^{RU} \left(\underline{\mathbf{H}}_{n,m,k}^{RU} \right)^H - \left(\mathbf{R}_{n,k}^{U,T_2} \right)^{-1} \mathbf{\Lambda}_m \left(\mathbf{R}_{n,k}^{U,T_2} \right)^{-H} \right\|_{\mathbb{F}}^2 \right\|_{\mathbb{F}}, \quad (2)$$

where $\mathbf{\Lambda}_0$ and $\mathbf{\Lambda}_m$ are diagonal matrices containing the diagonal elements of \mathbf{A}_0 and \mathbf{A}_m , respectively. Therefore, $\left(\mathbf{R}_{n,k}^{U,T_2} \right)^{-1}$ is the *jointly diagonalizing matrix* [17], while $\underline{\mathbf{H}}_{n,k}^{BU} \left(\underline{\mathbf{H}}_{n,k}^{BU} \right)^H$ and $\underline{\mathbf{H}}_{n,m,k}^{RU} \left(\underline{\mathbf{H}}_{n,m,k}^{RU} \right)^H$, $\forall m$ are the matrices to be diagonalized. Thus, the algorithm presented in [17] for solving (2) may be invoked at UE k for obtaining $\mathbf{R}_{n,k}^{U,T_2}$, which may be further fed back to the BS and RNs. Hence, the BS and RNs do not have to share $\underline{\mathbf{H}}_{n,k}^{BU}$ or $\underline{\mathbf{H}}_{n,k}^{RU}$ via the wireless channel and do not have to solve (2) again. As a result, we accomplish the goal of creating effective channel matrices that contain rows aiming to satisfy (1). Additionally, the columns of $\mathbf{R}_{n,k}^{U,T_2}$ have been normalized so that the power assigned for each SMC remains unaffected.

After obtaining the receive-BF matrix, the SMCs of the transmissions to UE k on subcarrier block n are given by the non-zero rows of the effective channel matrices $\underline{\mathbf{H}}_{n,k}^{BU,T_2}$ and $\underline{\mathbf{H}}_{n,m,k}^{RU,T_2}$, $\forall m$. Since the BS and the RNs act as distributed broadcasters in the second phase, they are only capable of employing *separate* ZFBF transmit matrices to ensure that none of them imposes interference on the SMCs it does not explicitly intend to serve. By employing one of the grouping

algorithms described in Section IV, the BS schedules $Q_j^{T_2} \leq \min \left[\min(N_B, N_R), \sum_{i=1}^K L_i^B + L_i^R \right]$ SMCs to serve simultaneously in the second phase, where L_i^B and L_i^R represent the number of SMCs of UE i served by the BS and by RNs in this phase, respectively, where we have $L_i^B + L_i^R \leq N_U$, $L_i^B \leq \min(N_B, N_U)$, and $L_i^R \leq \min(N_R, N_U)$. Let us denote the *refined* effective DL channel matrices, from the perspectives of the BS and RN m , consisting of the $Q_j^{T_2}$ selected SMCs as $\underline{\mathbf{H}}_{n,j}^{B,T_2}$ and $\underline{\mathbf{H}}_{n,j,m}^{R,T_2}$, respectively. Since these are known to each transmitter, they may employ ZFBF transmit matrices in the second phase, given by the right inverses $\mathbf{T}_{n,j}^{B,T_2} = \left(\underline{\mathbf{H}}_{n,j}^{B,T_2} \right)^H \cdot \left[\underline{\mathbf{H}}_{n,j}^{B,T_2} \left(\underline{\mathbf{H}}_{n,j}^{B,T_2} \right)^H \right]^{-1}$ for the BS, and $\mathbf{T}_{n,j,m}^{R,T_2} = \left(\underline{\mathbf{H}}_{n,j,m}^{R,T_2} \right)^H \cdot \left[\underline{\mathbf{H}}_{n,j,m}^{R,T_2} \left(\underline{\mathbf{H}}_{n,j,m}^{R,T_2} \right)^H \right]^{-1}$ for RN m . Similar to the first transmission phase, these ZFBF transmit matrices are normalized by $\mathbf{W}_{n,j}^{BU,T_2}$ and $\mathbf{W}_{n,j,m}^{RU,T_2}$, respectively, to ensure that each SMC transmission is initially set to unit power. Upon obtaining the selected SMCs, we denote the effective CNRs in the second transmission phase as $G_{n,j,e_2}^{BU,T_2} = \left| w_{n,j,e_2}^{BU,T_2} \right|^2 / \Delta\gamma N_0 W$ and $G_{n,j,e}^{RU,T_2} = \left| w_{n,j,e}^{RU,T_2} \right|^2 / \Delta\gamma N_0 W$, where w_{n,j,e_2}^{BU,T_2} and $w_{n,j,e}^{RU,T_2}$ are the diagonal elements in $\mathbf{W}_{n,j}^{BU,T_2}$ and $\mathbf{W}_{n,j,\mathcal{M}(e)}^{RU,T_2}$, respectively, and the subscript $\mathcal{M}(e)$ has been defined in Section III-A. To elaborate, for a second-phase BS-to-UE link, w_{n,j,e_2}^{BU,T_2} corresponds to SMC group j and subcarrier block n , while the subscript $e_2 \in \{0, \dots, \min[N_B, K \cdot \min(N_B, N_U)]\}$ is employed for further distinguishing the multiple selected SMCs associated with UEs from the BS. Similarly, $w_{n,j,e}^{RU,T_2}$, which also corresponds to SMC group j and subcarrier block n , is associated with the second-phase RN-to-UE link between RN $\mathcal{M}(e)$ and the particular UE of SMC-pair e .

IV. SEMI-ORTHOGONAL GROUPING ALGORITHMS

As described in Section II, the BS has to choose $Q_j^{T_1}$ and $Q_j^{T_2}$ SMCs for the first and second transmission phases, respectively. These selected SMCs collectively form the SMC group j . Since the system supports both direct and relaying links, the grouping algorithms described in [7], [8], which were designed for MIMO systems dispensing with relays, may not be directly applied. Instead, we propose a pair of viable grouping algorithms, namely the exhaustive search-based grouping algorithm (ESGA), and the orthogonal component-based grouping algorithm (OCGA).

Furthermore, for greater flexibility in forming viable SMC groups, additional SMCs may be considered in the second transmission phase, when tentatively assuming that only a subset of transmitters are activated. By employing this full list of SMCs, the system can achieve a higher performance.

In both grouping algorithms, each particular SMC must be evaluated before it may be included into the SMC group to be generated. This evaluation process is completed by the *SMCCheck*⁶ algorithm, which ensures that the SMC to be grouped satisfies the semi-orthogonality criterion of (1), while the transmit and receive dimensions of all nodes and the maximum spatial multiplexing gains of both transmission phases are not exceeded.

Algorithm 1: Exhaustive search-based grouping algorithm (ESGA)

inputs : set of SMC groups associated with subcarrier block n (initialized as empty set), \mathcal{G}_n
current SMC group (initialized as empty set), $\mathcal{E}_{n,j}$
SMCs associated with subcarrier block n , \mathcal{E}_n
semi-orthogonality parameter α

outputs: none

```

1 void ESGA ( $\mathcal{G}_n, \mathcal{E}_{n,j}, \mathcal{E}_n, \alpha$ )
2 begin
3   foreach  $e_c \in \mathcal{E}_n$  do
4     if SMCCheck ( $e_c, \mathcal{E}_{n,j}, \alpha$ ) then
5        $\mathcal{E}'_{n,j'} \leftarrow \mathcal{E}_{n,j} \cup \{e_c\}$ ;
6        $\mathcal{G}_n \leftarrow \mathcal{G}_n \cup \{\mathcal{E}'_{n,j'}\}$ ;
7       ESGA ( $\mathcal{G}_n, \mathcal{E}'_{n,j'}, \mathcal{E}_n \setminus e_c, \alpha$ );
8     end if
9   end foreach
10  return;
11 end

```

Algorithm 2: Orthogonal component-based grouping algorithm (OCGA)

inputs : set of SMC groups associated with subcarrier block n (initialized as empty set), \mathcal{G}_n
current SMC group (initialized as empty set), $\mathcal{E}_{n,j}$
SMCs associated with subcarrier block n , \mathcal{E}_n
semi-orthogonality parameter α

outputs: none

```

1 void OCGA ( $\mathcal{G}_n, \mathcal{E}_{n,j}, \mathcal{E}_n, \alpha$ )
2 begin
3   complete  $\leftarrow$  true;
4    $\mathcal{E}_c \leftarrow \{\}$ ;
5   foreach  $e_c \in \mathcal{E}_n$  do
6     if SMCCheck ( $e_c, \mathcal{E}_{n,j}, \alpha$ ) then
7       if  $|\mathcal{E}_{n,j}| == 0$  then
8          $\mathcal{E}'_{n,j'} \leftarrow \mathcal{E}_{n,j} \cup \{e_c\}$ ;
9         OCGA ( $\mathcal{G}_n, \mathcal{E}'_{n,j'}, \mathcal{E}_n \setminus e_c, \alpha$ );
10        return;
11       else
12          $\mathcal{E}_c \leftarrow \mathcal{E}_c \cup \{e_c\}$ ;
13         complete  $\leftarrow$  false;
14       end if
15     end if
16   end foreach
17   if complete then
18      $\mathcal{G}_n \leftarrow \{\mathcal{E}_{n,j}\}$ ;
19   else
20      $\mathcal{E}'_{n,j'} \leftarrow \mathcal{E}_{n,j} \cup \arg \max_{e_c \in \mathcal{E}_c} \text{NOC} (e_c, \mathcal{E}_{n,j})$ ;
21     OCGA ( $\mathcal{G}_n, \mathcal{E}'_{n,j'}, \mathcal{E}_n \setminus e_c, \alpha$ );
22   end if
23   return;
24 end

```

A. ESGA and OCGA

We present our first grouping method in Algorithm 1. Simply put, the ESGA recursively creates new SMC groups by exhaustively searching through all the possible combinations of SMCs and including those that pass the SMC checking algorithm. To elaborate, in the loop ranging from line 3 to line 9, the algorithm searches through all the possible SMCs associated with subcarrier block n , which are collectively denoted by \mathcal{E}_n and satisfy $e_c \in \mathcal{E}_n$. The specific SMCs that satisfy the checks performed in line 4 are appended to the current SMC group in line 5, and the resultant updated SMC group $\mathcal{E}'_{n,j'}$ is appended to the set of SMC groups obtained for subcarrier block n in line 6. Additionally, $\mathcal{E}'_{n,j'}$ is used recursively in line 7 for filling this group and for forming new groups. The computational complexity of ESGA is dependent on the number of SMCs which are semi-orthogonal to each other. The worst-case complexity is obtained when every SMC satisfies the checks performed in line 4, leading to a time-complexity (in terms of the number of SMC groups generated) upper-bounded (not necessarily tight) by $\mathcal{O}\left(\sum_{n=1}^N |\mathcal{E}_n|^\theta\right)$, where $\theta = \min[N_B, K \cdot \min(N_B, N_U) + M \cdot \min(N_B, N_R)] + \min\left[\min(N_B, N_R), \sum_{i=1}^K L_i^B + L_i^R\right]$.

In other words, each subcarrier block may be treated independently. For each subcarrier block, $|\mathcal{E}_n|$ SMCs must be checked until the maximum multiplexing gain in both the first and second phases has been attained.

The second algorithm, OCGA, is presented in Algorithm 2, which aims to be a lower complexity alternative to ESGA. The OCGA commences by creating a SMC candidate set \mathcal{E}_c , whose elements satisfy the checks performed in the *SMCCheck* algorithm, in lines 4 to 16. More specifically, if the current SMC group $\mathcal{E}_{n,j}$ is empty, the algorithm can simply create a new SMC group containing only the candidate SMC that has passed the *SMCCheck* algorithm in lines 7 to 10. If the SMC group is not empty, the algorithm adds to it the particular SMC candidate that results in the highest norm of the orthogonal component (NOC), via the Gram-Schmidt procedure [7], [8], in line 20. This process is repeated until the maximum multiplexing gain in both the first and second phases has been attained. When comparing the NOCs obtained for the relaying links, the minimum of the NOCs obtained from the BS-to-RN and RN-to-UE SMCs is used. This is because the information conveyed on the relaying link is limited by the weaker of the two transmissions, which is reflected in the effective channel gains quantified by these norms. If no SMCs satisfy the checks of line 6, the current SMC group is complete, and it is appended to the current set of SMC groups in line 18. Since new groups are only created when the current SMC group is empty, this algorithm results in much fewer groups than ESGA. The algorithmic time-complexity is given by $\mathcal{O}\left(\sum_{n=1}^N |\mathcal{E}_n|\right)$ as a single group is created for each initially-selected SMC.

Both grouping algorithms may be initialized with an empty SMC group, $\mathcal{E}_{n,j} \leftarrow \{\}$, and an empty set of SMC groups, $\mathcal{G}_n \leftarrow \{\}$, so that they recursively create and fill SMC groups according to their criteria. Additionally, a final step is performed to remove the specific groups, which result in effective channel gains that are less than or equal to that of another group, while having the same transmitters.

TABLE I: Simulation parameters used to obtain all results in Section V unless otherwise specified.

Simulation parameter	Value
Subcarrier block bandwidth, W [Hertz]	180k
Antenna configuration, (N_B, N_R, N_U)	(4, 4, 2)
Cell radius, [km]	{0.75, 1.75}
Ratio of BS-to-RN distance to the cell radius	0.5
SNR gap of wireless transceivers, $\Delta\gamma$ [dB]	0
Noise power spectral density, N_0 [dBm/Hz]	-174
Number of channel samples	10^4

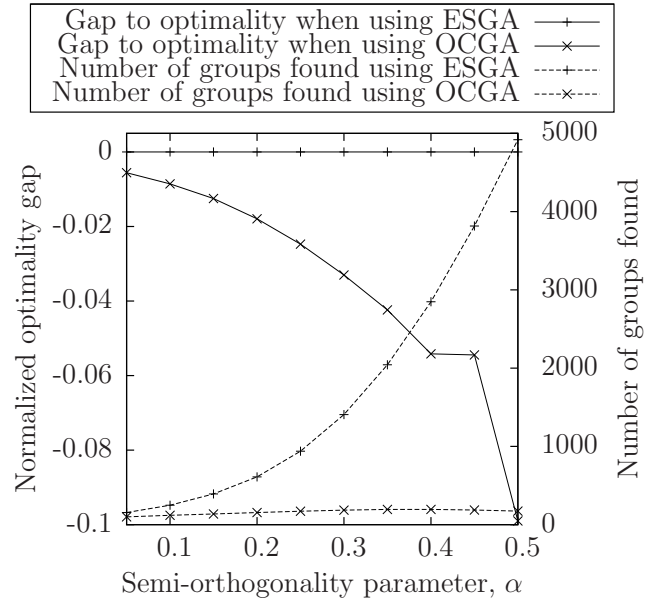


Fig. 2: The optimality gap and total number of SMC groups found when employing the ESGA and OCGA, and using the parameters in Table I with $N = 6$, $K = 2$, $M = 2$, $P_{max}^B = 20$ dBm, $P_{max}^R = 10$ dBm and a cell radius of 0.75km.

Therefore, this final step does not reduce the attainable system performance, but reduces the number of possible groups, thus alleviating computational complexity.

V. NUMERICAL RESULTS AND DISCUSSIONS

This section presents the numerical results obtained, when employing the grouping algorithms described in Section IV to the MIMO-OFDMA multi-relay cellular network considered. The pertinent simulation parameters are given in Table I. Additionally, the path-loss effect is characterized relying on the method and parameters of [15], where the BS-to-UE and RN-to-UE links are assumed to be non-line-of-sight (NLOS) links, since these links are typically blocked by buildings and other large obstructing objects, while the BS-to-RN links are realistically assumed to be line-of-sight (LOS) links, as the RNs may be strategically deployed on tall buildings to create strong wireless backhaul links. Furthermore, independently and randomly generated set of UE locations as well as fading channel realizations were used for each channel sample.

A. On the optimality and the relative complexity of ESGA and OCGA for various α values

Firstly, the behavior of the ESGA and OCGA as a function of α is examined. Note that in Fig. 2 the optimal system capacity is attained, when employing the maximization algorithm of [1], since the ESGA is capable of enumerating all possible SMC groupings satisfying (1) for the corresponding α . The 'normalized optimality gap' is then defined as $(\beta/\beta^*) - 1$, where β^* is the optimal capacity obtained from employing

⁶More details related to this algorithm may be found in [1].

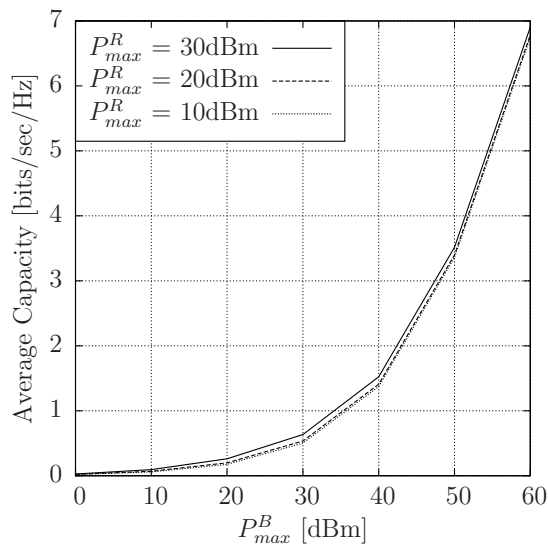
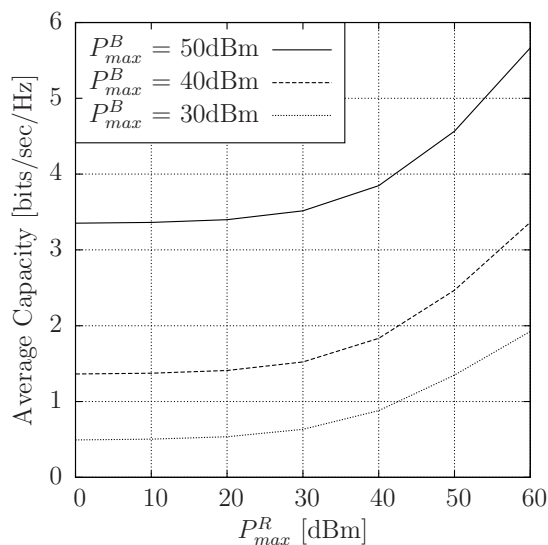
(a) Average achievable capacity for varying P_{max}^B .(b) Average achievable capacity for varying P_{max}^R .

Fig. 3: The average achievable capacity of the OCGA with random group selection and equal power allocation. The parameters in Table I with $N = 6$, $K = 10$, $M = 2$, $\alpha = 0.1$ and a cell radius of 1.75km are used.

the ESGA algorithm, and β is the capacity obtained from (in this case) the OCGA algorithm. We can see from Fig. 2, that the normalized optimality gap of OCGA relative to ESGA is about $-0.005 \sim -0.1$ for the α values considered. However, the number of groups found using ESGA is exponentially increasing with α . By contrast, for OCGA, this number is always significantly lower and gradually becomes less than 200, when α increases to 0.5. In fact, the number of groups found by OCGA is reduced to about 3.5% of that found by ESGA at $\alpha = 0.5$. This demonstrates the viability of employing OCGA as a reduced-complexity near-optimum alternative to ESGA.

B. The variation in achievable capacity for different values of P_{max}^B and P_{max}^R

As shown in Fig. 3(a), the achievable capacity is monotonically increasing with P_{max}^B and P_{max}^R , when employing the OCGA in conjunction with random group selection and equal power allocation. This is expected, since the capacity is a monotonically increasing function of the assigned power. Furthermore, it is clear that the effect of increasing P_{max}^B on the capacity is significantly more pronounced, than that of applying the same increase to P_{max}^R . The intuitive reasoning

behind this is that the power available at the BS has a more pronounced effect on the system's performance, since the direct links and, more importantly, the BS-to-RN links rely on the BS. Therefore, increasing P_{max}^R is futile, if the BS-to-RN links are not allocated sufficient power to support the RN-to-UE links.

VI. CONCLUSIONS

In this paper, a novel transmission protocol based on joint transmit-BF and receive-BF was developed for the multi-relay MIMO-OFDMA cellular network considered. By employing this protocol, the MIMO channel matrices were mathematically decomposed into several SMCs, which may be grouped for transmission to attain a high multiplexing gain. Therefore, we proposed both an exhaustive grouping algorithm and a lower-complexity alternative. These algorithms were evaluated based on their performance versus complexity trade-off. Furthermore, our additional results demonstrated the different effects that the available power at the BS and the RNs have on the system's capacity.

REFERENCES

- [1] K. Cheung, S. Yang, and L. Hanzo, "Spectral and energy spectral efficiency optimization of joint transmit and receive beamforming based multi-relay MIMO-OFDMA cellular networks," *IEEE Transactions on Wireless Communications*, vol. 13, no. 11, pp. 6147–6165, Nov. 2014.
- [2] M. Salem, A. Adinoyi, M. Rahman, H. Yanikomeroglu, D. Falconer, Y.-D. Kim, E. Kim, and Y.-C. Cheong, "An overview of radio resource management in relay-enhanced OFDMA-based networks," *IEEE Communications Surveys Tutorials*, vol. 12, no. 3, pp. 422–438, Apr. 2010.
- [3] L. Hanzo, Y. Akhtman, L. Wang, and M. Jiang, *MIMO-OFDM for LTE, WIFI and WIMAX: Coherent Versus Non-Coherent and Cooperative Turbo-Transceivers*. Wiley-IEEE Press, 2010.
- [4] G. Caire and S. Shamai, "On the achievable throughput of a multi-antenna Gaussian broadcast channel," *IEEE Transactions on Information Theory*, vol. 49, no. 7, pp. 1691–1706, Jul. 2003.
- [5] S. Vishwanath, N. Jindal, and A. Goldsmith, "Duality, achievable rates, and sum-rate capacity of Gaussian MIMO broadcast channels," *IEEE Transactions on Information Theory*, vol. 49, no. 10, pp. 2658–2668, Oct. 2003.
- [6] M. H. M. Costa, "Writing on dirty paper," *IEEE Transactions on Information Theory*, vol. 29, no. 3, pp. 439–441, May 1983.
- [7] T. Yoo and A. Goldsmith, "On the optimality of multi-antenna broadcast scheduling using zero-forcing beamforming," *IEEE Journal on Selected Areas in Communications*, vol. 24, no. 3, pp. 528–541, Mar. 2006.
- [8] N. Ul Hassan and M. Assaad, "Low complexity margin adaptive resource allocation in downlink MIMO-OFDMA system," *IEEE Transactions on Wireless Communications*, vol. 8, no. 7, pp. 3365–3371, Jul. 2009.
- [9] G. Raleigh and J. Cioffi, "Spatio-temporal coding for wireless communication," *IEEE Transactions on Communications*, vol. 46, no. 3, pp. 357–366, Mar. 1998.
- [10] K.-K. Wong, R. Murch, and K. Letaief, "A joint-channel diagonalization for multiuser MIMO antenna systems," *IEEE Transactions on Wireless Communications*, vol. 2, no. 4, pp. 773–786, Jul. 2003.
- [11] W. Ho and Y.-C. Liang, "Optimal resource allocation for multiuser MIMO-OFDM systems with user rate constraints," *IEEE Transactions on Vehicular Technology*, vol. 58, no. 3, pp. 1190–1203, Mar. 2009.
- [12] M. Sharif and B. Hassibi, "On the capacity of MIMO broadcast channels with partial side information," *IEEE Transactions on Information Theory*, vol. 51, no. 2, pp. 506–522, Feb. 2005.
- [13] G. Brante, I. Stupia, R. D. Souza, and L. Vandendorpe, "Outage probability and energy efficiency of cooperative MIMO with antenna selection," *IEEE Transactions on Wireless Communications*, vol. 12, no. 11, pp. 5896–5907, Nov. 2013.
- [14] A. Zappone, P. Cao, and E. Jorswieck, "Energy efficiency optimization in relay-assisted MIMO systems with perfect and statistical CSI," *IEEE Transactions on Signal Processing*, vol. 62, no. 2, pp. 443–457, Jan. 2014.
- [15] 3GPP, "TR 36.814 V9.0.0: further advancements for E-UTRA, physical layer aspects (release 9)," Mar. 2010.
- [16] J. Laneman, D. Tse, and G. Wornell, "Cooperative diversity in wireless networks: Efficient protocols and outage behavior," *IEEE Transactions on Information Theory*, vol. 50, no. 12, pp. 3062–3080, Dec. 2004.
- [17] A. Yeredor, "Non-orthogonal joint diagonalization in the least-squares sense with application in blind source separation," *IEEE Transactions on Signal Processing*, vol. 50, no. 7, pp. 1545–1553, Jul. 2002.